ScienceDirect
IFAC Papers Online
CONFERENCE PAPER ARCHIVE
IFAC PapersOnLine 50-1 (2017) 12210–12215

A Data-driven Gain Adaptation Mechanism for Flexible Usability in the UGent Knee Rig

Amélie Chevalier * **Brecht De Vlieger** * **Matthias Verstraete** **
Clara Ionescu * **Robin De Keyser** *

* *Ghent University, Department of Electrical energy, Systems and Automation, Research group of Dynamical Systems and Control (DySC), Belgium (e-mail: amelie.chevalier@ugent.be, claramihaela.ionescu@ugent.be, robain.dekeyser@ugent.be).*
** *Ghent University Hospital, Department of Physical Medicine and Orthopaedic Surgery, Belgium (e-mail: matthias.verstraete@ugent.be)*

Abstract: This paper presents a data-driven gain adaptation mechanism in order to make the usability of the UGent Knee Rig (UGKR) more flexible. The design of the UGKR is unique as it is characterized by a movable ankle joint contrary to traditional dynamic knee rigs which are used to investigate knee kinematics and surgical techniques. This feature allows the UGKR to perform both bicycle motions and squat motions while applying a quadriceps force and hamstring forces. The control of the UGKR is a model-based control strategy which requires time-consuming system identification for each new knee specimen. A data-driven gain adaptation mechanism is developed reducing the necessary time for identification creating a flexible usability. Two adaptation mechanisms are implemented and tested on both a mechanical hinge and a cadaver knee: a rectangular sequence and a polar sequence. The results from squat and bicycle tests indicate that rectangular sequence provides good performance for the rigid mechanical hinge, however, it fails for the elastic cadaver knee during full extension. It is shown that the polar sequence results in good performance for the cadaver knee compared to the rectangular mechanism.

Keywords: Automatic gain control, Adaptation, Biomedical control, Dynamic systems, Decoupling

1. INTRODUCTION

Dynamic knee rigs have been developed by Shaw and Murray (1973) to test in-vitro the feasibility of knee implants in cadaver specimens in order to validate proper functioning. Nowadays, dynamic knee rigs are also used in the assessment of surgical techniques by looking into the kinematics of the knee joint (Arnout et al., 2015). Based on these observations, the orthopedic researcher investigates the effect of the surgical technique on the post-operative stability of the knee joint for different types of knee implants. This post-operative instability is one of the main reasons why total knee replacement still fails today (Vince, 2014; Lombardi Jr. et al., 2014).

Most knee rigs which are found in literature are based on the Oxford Knee Rig (OKR) developed by Bourne et al. (1978). The OKR performs a squat movement by moving the hip joint vertically downwards, while the ankle joint is fixed in space. During this motion the natural six degrees of freedom of the knee joint are maintained (Zavatsky, 1997); nonetheless, the OKR has one major limitation: it can only perform squat motions. Although the squat motion is relevant as it is used in daily tasks, i.e. rising from a chair and descending a stair, a new type of knee rig has been developed in order to increase the flexibility in types of motions without increasing the cost of the rig significantly: the UGent Knee Rig (UGKR) (Verstraete and Victor, 2015).

The UGKR is capable of performing a bicycle motion while applying quadriceps and hamstring forces by moving the ankle joint in the sagittal plane while the hip joint is fixed (Chevalier et al., 2016). As the UGKR uses five different actuators to impose the desired motions and forces, the system is a multiple-input/multiple-output (MIMO) system. A decoupled PID control strategy is used to control the forces and position in the UGKR (Chevalier et al., 2016). The PID controllers are a model-based control strategy which uses a model to tune the control parameters. For the UGKR, this model is obtained trough a system identification technique called the prediction error method (Ljung, 1999). However, this identification method is time-consuming in the case of the UGKR due to many interactions and gain variability over the full range of motion. To overcome this limitation, we propose in this paper a data-driven gain adaptation mechanism which is experimentally validated.

This paper is structured as follows: section two provides a system description of the UGKR with the resulting transfer function models from identification. Section three presents the principles behind the new gain determination

10.1016/j.ifacol.2017.08.2339

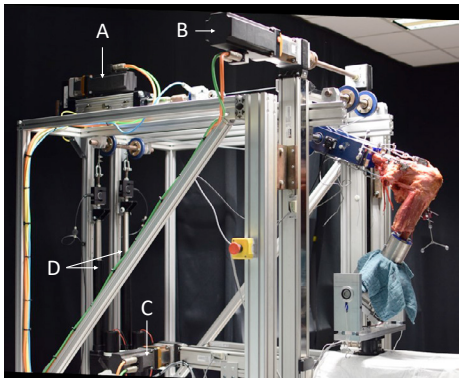

(a) The UGKR with a cadaver knee specimen inserted. A is the quadriceps actuator, B is the vertical actuator, C is the horizontal actuator and D are both hamstring actuators.

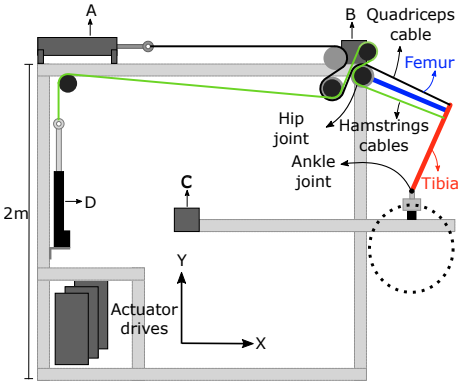

(b) Schematic representation of the UGKR. The coordinates of the hip joint in the XY coordinate system are (X=500,Y=1300).

Fig. 1. Photo of the UGKR and its corresponding schematic representation.

method and proposes two different gain determination sequences. The fourth section discusses two experiments and the results in order to investigate the performance of the controllers by using the proposed gain determination sequences. Tests are performed on both cadaver knee specimens and a mechanical hinge model. The fifth section finishes with some conclusions and future work.

2. SYSTEM DESCRIPTION

This section provides a short system description in order to understand the workings of the UGKR. For a more detailed system description, readers are referred to Verstraete and Victor (2015) and Chevalier et al. (2016).

The UGKR (Fig. 1a) is based on principles of the OKR developed by Bourne et al. (1978). Unlike the OKR, the hip joint in the UGKR is fixed while the ankle joint can move freely in the XY plane. The UGKR consists of five linear actuators imposing three different forces (i.e. quadriceps, medial hamstring, lateral hamstring) and two motions (i.e. vertical and horizontal) onto a knee specimen. Figure 1b shows a schematic representation of the UGKR which has a total height of 2 m. The quadriceps force is applied by actuator A connected by a cable-pulley system to the insertion point of the quadriceps muscle. Actuators B and C are respectively the vertical and horizontal positioning actuator for the ankle joint. Two actuators D are implemented to mimic the force of the hamstring muscles and are connected via two cable-pulley systems to the medial (i.e. inner) and lateral (i.e. outer) insertion points of the hamstring muscles.

The UGKR can be inserted with three types of specimens:

- a mechanical hinge model of the human knee,
- a sawbone model where a knee implant can be inserted, and
- a cadaver knee specimen.

Fig. 2 shows the controlled and manipulated variables in the UGKR together with the direct paths and the cross-interactions of this multiple-input/multiple-output (MIMO) system. A previous study on the system's dynamics has shown a strong cross-interaction between the input of the horizontal and vertical position actuators and the three output forces (Chevalier et al., 2016). Identification between the input voltages of the actuators and the output position and forces has been performed using the mechanical hinge model, resulting in a set of discrete time transfer functions with a sampling period of 30 ms, listed in Table 1 where the variable gains are listed in Table 2. Note that the direct paths (i.e. first five transfer functions in Table 1) have a constant gain, while the cross-interactions (i.e. last six transfer functions in Table 1) are characterized by a variable gain depending on the position of the ankle as shown in Table 2.

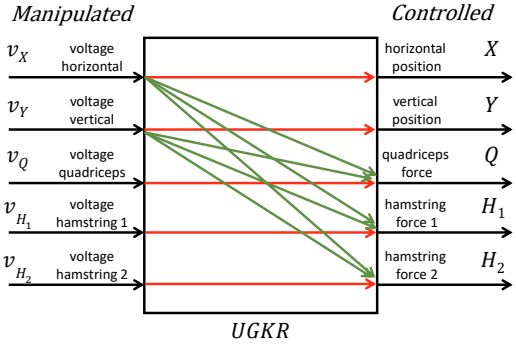

Fig. 2. Controlled and manipulated variables in the UGKR.

Table 1. Identified models; The corresponding gains are given in Table 2.

Model [unit]	Identification
G_{Xv_X} [mm/V]	$\frac{0.50z^{-3}}{1-z^{-1}}$
G_{Yv_Y} [mm/V]	$\frac{0.36z^{-4}}{1-z^{-1}}$
G_{Qv_Q} [N/V]	$\frac{15.83z^{-2}}{1-z^{-1}}$
$G_{H_1v_{H_1}}$ [N/V]	$\frac{4.54z^{-2}}{(1-z^{-1})(1-0.8z^{-1})}$
$G_{H_2v_{H_2}}$ [N/V]	$\frac{3.38z^{-2}}{(1-z^{-1})(1-0.77z^{-1})}$
G_{Qv_X} [N/V]	$\frac{K_{QX}z^{-2}}{1-z^{-1}}$
G_{Qv_Y} [N/V]	$\frac{K_{QY}z^{-2}}{1-z^{-1}}$
$G_{H_1v_X}$ [N/V]	$\frac{K_{H_1X}z^{-2}}{1-z^{-1}}$
$G_{H_1v_Y}$ [N/V]	$\frac{K_{H_1Y}z^{-2}}{1-z^{-1}}$
$G_{H_2v_X}$ [N/V]	$\frac{K_{H_2X}z^{-2}}{1-z^{-1}}$
$G_{H_2v_Y}$ [N/V]	$\frac{K_{H_2Y}z^{-2}}{1-z^{-1}}$

Table 2. Gain variations for the cross-interactions with X and Y expressed in mm

	K_{QX}			K_{QY}		
Y \ X	700	500	300	700	500	300
900	-9.53	-9.85	-6.21	-0.12	2.47	5.13
750	-7.77	-7.17	-4.59	1.92	3.25	5.00
600	-6.47	-5.71	-3.48	3.39	4.51	5.35
	K_{H_1X}			K_{H_1Y}		
Y \ X	700	500	300	700	500	300
900	0.42	-0.64	0.63	0.40	0.23	-0.11
750	0.44	0.55	0.59	0.36	0.37	0.01
600	0.39	0.38	0.50	0.35	0.36	0.25
	K_{H_2X}			K_{H_2Y}		
Y \ X	700	500	300	700	500	300
900	0.36	0.51	0.45	0.35	0.19	-0.08
750	0.36	0.44	0.41	0.25	0.23	0.04
600	0.24	0.37	0.39	0.25	0.32	0.16

In order to obtain these transfer function models, a total of 59 identifications were needed which takes about 2 hours (5 for the direct paths and 6× 9 for the cross-interactions with the variable gains). However, most experiments on the UGKR will use cadaver specimens and as there is a large inter-patient variability, this method of identification is unsuitable to perform on every new knee sample. The control strategy used to control the UGKR is a decoupled PID control strategy with feedforward action as presented by Chevalier et al. (2016) and for which the performance has been addressed in Chevalier et al. (submitted) (Fig. 3). As this strategy uses the variable gains in both the feedforward action as in the decouplers, a good gain estimation is important for the total control performance. Notice from Table 2 that the gain variability can vary up to 100% compared to the nominal value at coordinate (500,750). Therefore, this research investigates the possibility of using an automatic, data-driven gain determination sequence to complete the gain estimation task.

3. PROPOSED GAIN ADAPTATION MECHANISM

The main idea behind the gain determination sequence is to estimate the gains during a short pre-experiment run, where the ankle follows a certain trajectory. This sequence can then be done every time a new cadaver knee specimen is inserted into the UGKR. The first step is to find a simplified expression for the gain estimation based on simple voltage measurements. The second step consists of selecting suitable test conditions and trajectories within the range of motion of the UGKR.

3.1 Gain estimation procedure

The control scheme for the quadriceps force including the decouplers and the cross-interaction is shown in Fig. 3. Here, FF_i with $i = X, Y, Q, H_1, H_2$ represents the feedforward controller which is a differentiator multiplied with a gain in order to estimate the speed and express it as a voltage signal v_{Fi}. PID_i with $i = X, Y, Q, H_1, H_2$ is the PID controller with an output voltage v_{Ci}. De decouplers are denoted by D_{iX} and D_{iY}. A similar control architecture is implemented for both hamstring forces.

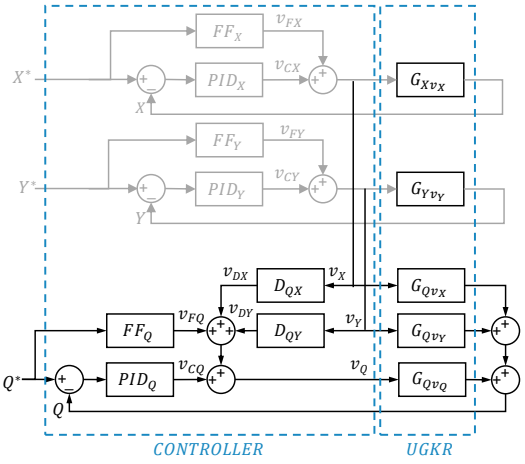

Fig. 3. Control scheme for the quadriceps (Q) control including decouplers and cross-interaction. Similar schemes are implemented for the hamstrings (H_1 and H_2).

From this scheme, the total control effort for the forces can be expressed as:

$$v_i = v_{Ci} + v_{Fi} + D_{iX} \cdot v_X + D_{iY} \cdot v_Y \quad \text{with } i = Q, H_1, H_2 \tag{1}$$

The decouplers are designed to cancel the cross-interactions and can therefore be expressed as:

$$D_{iX} = \frac{-G_{iv_X}}{G_{iv_i}} \text{ and } D_{iY} = \frac{-G_{iv_Y}}{G_{iv_i}} \quad \text{with } i = Q, H_1, H_2$$

For the quadriceps decoupler in the X-direction these expressions simplify to:

$$D_{QX} = \frac{-G_{Qv_X}}{G_{Qv_Q}} = \frac{-K_{QX}z^{-2}}{1-z^{-1}} \frac{1-z^{-1}}{15.83z^{-2}} = K_{DQX} \tag{2}$$

However, for the hamstring decouplers, these expressions are not simplified to a single gain.

$$D_{H_1X} = \frac{-G_{H_1v_X}}{G_{H_1v_{H_1}}} = \frac{-K_{H_1X}z^{-2}}{1-z^{-1}} \frac{(1-z^{-1})(1-0.8z^{-1})}{4.54z^{-2}}$$

For the gain adaptation mechanism, the dynamics of the decouplers can be neglected if the step response of the approximated system will result in the same gain. This can be seen in Fig. 4 which compares the step response of the original direct transfer function and the one of the following approximation:

$$G^*_{H_1v_{H_1}} = \frac{4.54z^{-2}}{(1-z^{-1})(1-0.8)} = \frac{22.7z^{-2}}{(1-z^{-1})}$$

From this figure it can be concluded that both step responses have the same slope in steady state. As the slope is directly linked to the gain, both systems will result in the same gain during the gain estimation procedure. The resulting hamstring decoupler is:

$$D_{H_1X} = \frac{-G_{H_1v_X}}{G^*_{H_1v_{H_1}}} = \frac{-K_{H_1X}}{22.7} = K_{DH_1X} \tag{3}$$

Similar reasoning is done for the second hamstring force, resulting in:

$$D_{H_2X} = \frac{-G_{H_2v_X}}{G^*_{H_2v_{H_2}}} = \frac{-K_{H_2X}}{14.7} = K_{DH_2X} \tag{4}$$

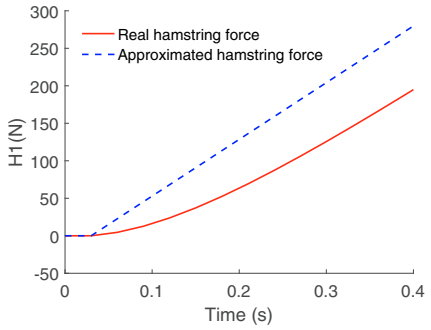

Fig. 4. Comparison between the step response of the original direct hamstring transfer function and its approximation.

Similar expressions as (2)-(4) are valid for the Y-direction. The total control effort expressed in (1), can now be simplified using equations (2)-(4) as:

$$v_i = v_{Ci} + v_{Fi} + K_{DiX} \cdot v_X + K_{DiY} \cdot v_Y \quad \text{with } i = Q, H_1, H_2$$

In order to estimate the values of K_{DiX} and K_{DiY} for $i = Q, H1, H2$, only one position actuator will move at a time and a constant force reference signal is applied. As the feedforward action is defined as a differentiator estimating the speed of the actuator piston from the reference force (Chevalier et al., 2016), the value for the signal v_{Fi} is zero at all times for a constant force reference signal. In the implemented control strategy, the PID controllers are only used to reject small errors on the feedforward control. The assumption is made that the feedforward control works perfectly, thus resulting in a zero control effort of the PID controllers v_{Ci}. With these assumptions the total control effort expressions, for the horizontal and vertical direction respectively, become:

$$v_i = K_{DiX} \cdot v_X$$
$$v_i = K_{DiY} \cdot v_Y \quad \text{with } i = Q, H_1, H_2$$

Following this reasoning, the gain of the decouplers in every position can be estimated as the ratio between the input to the force actuator and the input signal to the horizontal or vertical actuator for a test where only one actuator moves at a time and a constant force is applied. From these results, the gains of the cross-interactions can be obtained by multiplying them with the gain of the direct path of the corresponding force obtained from identification.

3.2 Test sequence

Rectangular sequence In order to apply the conditions which follow the reasoning in previous section, a test needs to be designed where the position actuators move only one at the time and the force is kept constant. The following gain adaptation sequence is proposed and illustrated in Fig. 5:

- Move the horizontal actuator at a constant velocity while the vertical actuator is kept at the same position 900 mm by sending in 0 V (from 1 to 2 in Fig. 5). The input to the actuator is a constant voltage signal v_X of 3 V.

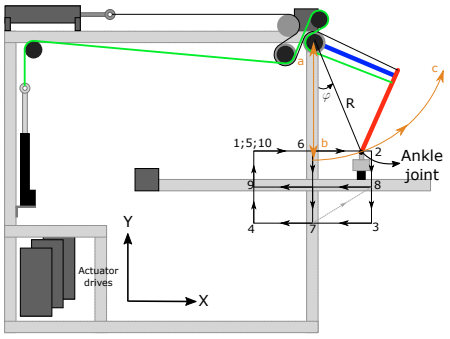

Fig. 5. Gain test sequences. (Rectangular test sequence in black (1-10), Polar test sequence in orange (a-c)).

- Use the PID controllers to keep the forces constant during the movement which will result in the control effort voltage signal v_i.
- The values for K_{DiX} are estimated by dividing v_i by v_X.

This sequence is repeated in the Y-direction and for different heights resulting in a rectangular trajectory as can be seen in Fig. 5.

A major limitation of the rectangular seuqence is that a part of the region covered during the bicycle motion is not covered during the gain determination sequence as it would lead to rupture of the knee specimen (Fig. 6 indicated by 'Problem area'). Gains outside of the rectangular sequence matrix are estimated using linear interpolation. Tests have shown that in this lowest region where the knee is almost fully extended, the absolute value of the gain increases rapidly (Fig. 7). This error on the gain determination in the rectangular sequence will lead to poor tracking performance of the controllers (see section Results).

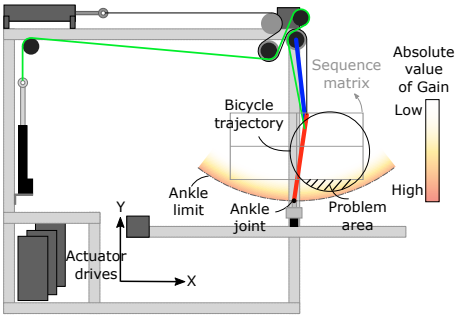

Fig. 6. Limitations on rectangular calibration.

Polar sequence Due to the limitations of the rectangular sequence, a second test sequence has also been applied which uses polar coordinates. The polar trajectory is based on the same principle as the rectangular sequence: only one variable at the time is changing. Therefore, two experiments need to be performed in the polar sequence: i) an angular change and ii) a radial change. For the angular change, the following sequence is applied only once:

- The ankle performs quarter of a circle (Fig.5 b to c) with a fixed radius of 500 mm while the speed normal to the circular trajectory remains constant.

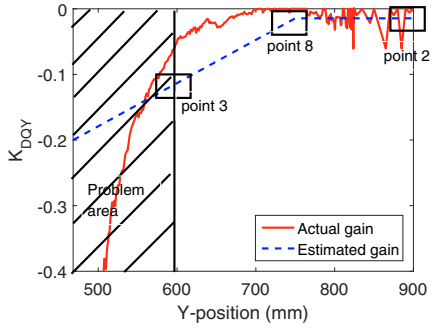

Fig. 7. Comparision between linear interpolated decoupler gain and the actual decoupler gain for a fixed X-value of 700 mm. The corresponding points from Fig. 5 are indicated on the plot. The problem area is also indicated.

- Use the PID controllers to keep the forces constant during the movement which will result in the control effort voltage signal v_i.
- The values for the angular gain K_{iN} with $i = Q, H_1, H_2$ are estimated by dividing v_i by the input voltage in the normal direction v_N which is expressed as:

$$v_N = \frac{K_{Xv_X}}{K_{Yv_Y}} \cdot u_X \cdot \cos\varphi + u_Y \cdot \sin\varphi$$

with K_{Xv_X} and K_{Yv_Y} respectively the gain of G_{Xv_x} and G_{Yv_Y} and φ the angle defined in Fig. 5. Note here that the obtained gain will only depend on the radius and is independent of the type of specimen inserted into the UGKR as only a rotation around the hip joint is performed. The resulting values for a radius of 500 mm are 0.33, -0.08 and -0.08 respectively for K_{QN}, K_{H_1N} and K_{H_2N}. By scaling this value with a factor of $500/R$, the value of the gain can be obtained for any radius R.

For the radial change, the following sequence is applied for each new specimen:

- The ankle performs a squat experiment where the ankle remains under the hip joint (Fig.5 a to b). During this experiment the speed in the radial direction is equal to the speed in the vertical direction and is constant. This implies that the input voltage to obtain a change in radial direction is equal to the input voltage to the Y-actuator v_Y.
- Use the PID controllers to keep the forces constant during the movement which will result in the control effort voltage signal v_i.
- The values for the radial gain K_{iR} with $i = Q, H_1, H_2$ are estimated by dividing v_i by v_Y.

4. RESULTS AND DISCUSSION

A first experiment is performed to evaluate the performance of the rectangular gain determination sequence. A bicycle motion is performed with a radius of 170 mm and a period of 10 s as illustrated in Fig. 1b. Both hamstring forces are kept constant 100 N during the experiment and the quadriceps reference signal (Fig. 8a) is created using a finite element simulator called AnyBody (Anybody Technology, 2016). The gain determination sequence only

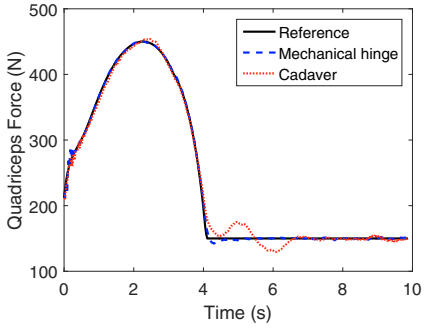

(a) Quadriceps tracking during a bicycle motion for a mechanical hinge vs a cadaver using the rectangular sequence.

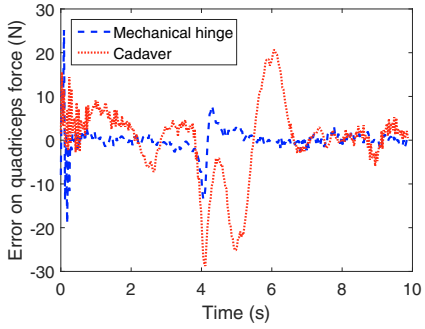

(b) Error on the quadriceps force during a bicycle motion for a mechanical hinge vs a cadaver using the rectangular sequence.

Fig. 8. Results for the performance of the rectangular sequence.

has effect on the gain of the decouplers used in the force control, the type of sequence chosen will not have an effect on the tracking performance of the positioning controllers. For the results on the position tracking performance, the reader is referred to Chevalier et al. (2016).

Fig. 8a depicts the reference signal and the output signals for the quadriceps force during one bicycle motion for a mechanical hinge and a cadaver. Notice that the reference signal remains constant after half a circle as than the second leg is supposed to deliver the necessary force and the UGKR is designed to mimic the motion of one leg. Notice that the mechanical hinge model has a relatively good tracking performance compared to the cadaver knee. With the cadaver knee inserted, the UGKR has difficulty following the constant reference signal of the quadriceps force. The errors between the quadriceps force and the reference signal are given in Fig. 8b. Notice that the error for the cadaver knee is significantly bigger than the error for the mechanical hinge. It can be concluded that the rectangular gain determination sequence leads to good results for the mechanical hinge which is very rigid in design and will therefore have fewer fluctuations in the gain. However, for the cadaver knee, which is more flexible and thus experiences more gain variations, the rectangular sequence is insufficient. Therefore, the polar sequence has been proposed in Section 3.

To overcome the limitation of the rectangular sequence, a second experiment is performed to test the polar gain determination sequence for the cadaver knee. To show the

versatility of the UGKR, a squat movement is performed during this experiment where the ankle joint moves vertically down over a length of 365 mm in 10 s and then goes back up to its original position during another 10 s. The applied quadriceps force during this squat is a sinusoidal signal as can be seen in Fig. 9a. A comparison of the actual force output signals between the rectangular sequence and the polar sequence is also shown in Fig. 9a. Note here that the tracking performance of the force with the rectangular sequence is greatly diminished in the region where the knee is almost in complete extension (Recall the discussion from Section 3). This observation is supported by the evolution of the error between the force reference and the actual force given in Fig. 9b. Note that in this region, between 7.5 s and 12.5 s, the polar sequence provides an improved tracking performance compared to the rectangular sequence. The mean value of the absolute error between 7.5 s and 12.5 s reduces from 27.39 N to 0.25 N for respectively the rectangular and the polar sequence.

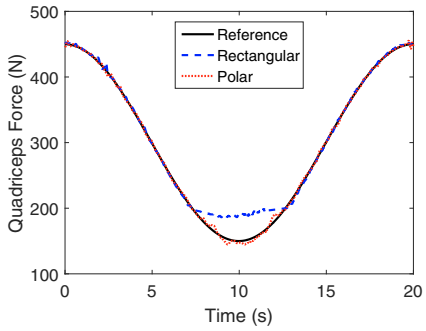

(a) Quadriceps tracking during a squat motion on a cadaver knee for the rectangular vs the polar sequence.

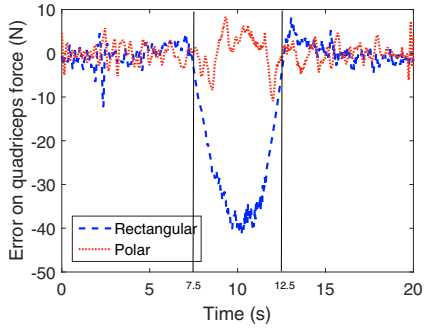

(b) Error on the quadriceps force during a squat motion on a cadaver knee for the rectangular vs the polar sequence.

Fig. 9. Results for the performance of the polar sequence.

5. CONCLUSION

This research discusses a data-driven gain determination mechanism for the UGent Knee Rig (UGKR). Due to the model-based control, time consuming identification is needed to tune the control structure. This disadvantage has been addressed here by implementing a gain estimation mechanism to estimate the variable gains. Two types of sequences are investigated: i) a rectangular sequence and ii) a polar sequence. The proposed gain adaptation mechanism is validated during two experiments with both mechanical hinge models and cadaver knee specimens. The results show that the rectangular gain determination yields a good force tracking performance for the mechanical hinge which is rigid. However, for the cadaver knee which is more flexible this sequence results in significant errors. The polar sequence is proven to be more successful for the gain determination of the cadaver knee.
Future work consists of i) a comparison of the obtained gains for knee specimens from different patients to quantify the inter-patient variability and ii) a comparison between the left and right knee of the same patient to quantify the intra-patient variability.

ACKNOWLEDGEMENTS

C. M. Ionescu acknowledges the Flanders Research Center (FWO) grant no. 12B3415N for its financial support. M. Verstraete acknowledges the Flanders Research Center (FWO) grant no. 12N5117N for its financial support. A. Chevalier, C.M. Ionescu and R. De Keyser are members of the Flanders Make consortium, group EEDT.

REFERENCES

Anybody Technology (2016). Anybody software. `http://www.anybodytech.com/`, accessed 25th of October 2016.

Arnout, N., Vanlommel, L., Vanlommel, J., Luyckx, J., Labey, L., Innocenti, B., Victor, J., and Bellemans, J. (2015). Post-cam mechanics and tibiofemoral kinematics: a dynamic in vitro analysis of eight posterior-stabilized total knee designs. *Knee surgery sports traumatology arthroscopy*, 23(11), 3343–3353.

Bourne, R., Goodfellow, J., and O'Connor, J. (1978). A functional analysis of various knee arthroplasties. *Transactions of the 24th Annual Meeting of the Orthopaedic Research Society*, 24, 160.

Chevalier, A., De Vlieger, B., Verstraete, M., Ionescu, C., and De Keyser, R. (2016). Decoupled PID control with gain adaptation for a cycling dynamic knee rig. In *Proc. International Conference on Systems, Man and Cybernetics (SMC, Budapest, Hungary, Oktober 2016)*, 2779–2784.

Chevalier, A., Verstraete, M., Ionescu, C., and Keyser, R.D. (submitted). A decoupled control strategy for the ugent knee rig: Design, implementation and validation. *IEEE/ASME Transactions on Mechatronics*.

Ljung, L. (1999). *System Identification: Theory for the User*. Prentice Hall.

Lombardi Jr., A., Berend, K., and Adams, J. (2014). Why knee replacements fail in 2013: Patient, surgeon, or implant? *The Bone & Joint Journal*, 96(11), 101–104.

Shaw, J.A. and Murray, D.G. (1973). Knee joint simulator. *Clinical Orthopaedics and Related Research*, 94, 15–23.

Verstraete, M. and Victor, J. (2015). Possibilities and limitations of novel in-vitro knee simulator. *Journal of Biomechanics*, 42(12), 3377–3382.

Vince, K. (2014). The problem total knee replacement: Systematic, comprehensive and efficient evaluation. *The Bone & Joint Journal*, 96(11), 105–111.

Zavatsky, A.B. (1997). A kinematic-freedom analysis of a flexed-knee-stance testing rig. *Journal of Biomechanics*, 30(3), 277–280.